Vol. 535: 161–176, 2015
doi: 10.3354/meps11373

MARINE ECOLOGY PROGRESS SERIES
Mar Ecol Prog Ser

Published September 15

Effects of larval swimming behavior on the dispersal and settlement of the eastern oyster *Crassostrea virginica*

Alfred B. Hubbard, Matthew A. Reidenbach*

Department of Environmental Sciences, University of Virginia, Charlottesville, Virginia 22904, USA

ABSTRACT: Large-scale efforts to restore oyster (*Crassostrea virginica*) habitat rely on the creation of high-relief hard substrate to improve the natural recruitment of larvae originating from existing oyster populations. Delivery of competent larvae to reefs is influenced by larval behavior, which respond to elevated levels of turbulence by a downward swimming behavior. To determine the geographic dispersal of populations of oyster larvae and how swimming behavior of larvae alters settlement patterns within Virginia (USA) coastal bays, this study utilized a depth-averaged Delft3D© hydrodynamic model coupled to a larval behavior model which incorporates an increased downward swimming speed in response to elevated turbulence. Turbulence and flow measurements over oyster reefs, oyster restoration sites, and bare seafloor were quantified using velocimeters. Hydrodynamic cues were input into the larval behavior model to determine how changes in swimming behavior due to turbulence influence settlement patterns. Results indicate that alterations in settlement velocity, specifically maintaining approximate neutral buoyancy until larvae are both mature and over an existing reef, substantially increased the probability of settling on suitable substrate. We also found that oyster reefs in low velocity regions have a higher probability of self-colonization, while reefs found in less sheltered higher velocity environments receive comparatively little of their own larvae and depend upon connectivity with other areas. Data from *in situ* larval settlement plates agree with model results and indicate that rates of settlement are ~1.5 to 3× greater over existing reefs composed of primarily vertically oriented oysters than over restoration reefs that are less topographically complex.

KEY WORDS: Oyster · Larval dispersal · Settlement behavior · *Crassostrea virginica*

INTRODUCTION

Crassostrea virginica, the eastern oyster, is a filter-feeding bivalve that has historically been a very important species in the Chesapeake Bay estuary and mid-Atlantic coast. *C. virginica* forms complex reefs that increase estuarine biodiversity by providing habitat for fish and invertebrates (Lenihan & Peterson 1998), as well as improving the commercial value of local fisheries (Breitburg et al. 2000). Oysters also decrease turbidity and improve water quality through active filtration of algae and detritus (Newell 1988, Nelson et al. 2004, Reidenbach et al. 2013). Unfortunately, the total biomass of the eastern oyster in Chesapeake Bay and coastal waters is estimated to be 1% of its historical maximum due to overharvesting, disease, and poor management (Rothschild et al. 1994, Kemp et al. 2005). *C. virginica* is now targeted for restoration efforts (Cerco & Noel 2007, Schulte et al. 2009), which include construction of artificial structures designed to simulate mature oyster reefs and facilitate larval settlement (Nestlerode et al.

*Corresponding author: reidenbach@virginia.edu

2007). Along the Virginia, USA, coastline, The Nature Conservancy has constructed multiple oyster restoration reefs (Fig. 1), using deposited shell consisting of *C. virginica* oyster shell and larger *Busycotypus canaliculatus* whelk shell to create high-relief hard substrate to enhance recruitment of oyster larvae (Whitman & Reidenbach 2012). The success of these restoration efforts partly relies on adequate transport and recruitment of oyster larvae to restoration areas.

Although dispersal of larvae is primarily driven by oceanographic, tidal, and other coastal currents, larval behavior can control local settlement patterns through specific responses to a variety of settlement cues, which include responses to salinity, light, dissolved chemicals, and turbulence (Carriker 1951, Wood & Hargis 1971, Butman 1987, Finelli & Wethey 2003, Hadfield & Koehl 2004). *C. virginica* are sessile as adults and have a planktonic larval stage. Free-swimming mature larvae typically do not exceed swimming speeds of 3 mm s^{-1}. However, rapid downward swimming in response to settlement cues can periodically exceed these levels (Hidu & Haskin 1978, Fuchs et al. 2013), significantly influencing patterns of dispersal (North et al. 2008).

For new reefs to develop, oysters must survive a planktonic larval stage that lasts several weeks, attach to substrate, and grow from spat to large individuals. Reproduction of *C. virginica* typically begins when the water temperature reaches 25°C (Galtsoff 1964). The larvae require ~14 d in the water column to mature. In this 2 wk period from the time of fertilization, planktonic larvae pass through stages designated as early umbo, late umbo, mature, and eyed larvae. Once mature, and after the ~14 d planktonic time period, the larvae have ~7 more days to find suitable substrate or else they die (Kennedy 1996). Eyed larvae are ~200 to 300 µm in diameter (Carriker 1951). After attachment to substrate, eyed larvae cement themselves to hard surfaces and are then known as spat.

Larvae preferentially settle gregariously on hard, stable substrates that are ideally composed of mature oyster beds with high vertical relief (Schulte et al. 2009, Whitman & Reidenbach 2012). They swim downwards in response to chemical and turbulence cues from oyster beds (Tamburri et al. 1996, Fuchs et al. 2013), and will swim back up into the water column if deposited on undesirable substrate (Turner et al. 1994). Larvae can determine whether they are over reef areas by sensing an increase in turbulence within the water column (Fuchs et al. 2013), which can be induced by the enhanced roughness of the reef (Whitman & Reidenbach 2012, Reidenbach et al. 2013). The magnitude of turbulence necessary for planktonic larvae to respond with a change in downward swimming velocity was characterized in laboratory experiments by Fuchs et al. (2013), who found that settlement velocity was best explained in relation to the dissipation rate of turbulent kinetic energy, ε. Vertical swimming velocities attributed to this behavior range from near-zero velocities in calm water to downward swimming velocities of 1.8 cm s^{-1} in strong turbulence ($\varepsilon > 7.1 \times 10^{-2}$ cm^2 s^{-3}). Active larval behavior determining where larvae settle has been reviewed by Butman (1987) and Eckman et al. (1994), and has been described more recently by Fuchs et al. (2004) and DiBacco et al. (2011). In addition, active downward swimming, which has been found in mollusc larvae (Hadfield & Koehl 2004, Koehl & Reidenbach 2007, Fuchs et al. 2013), is substantially greater than passive

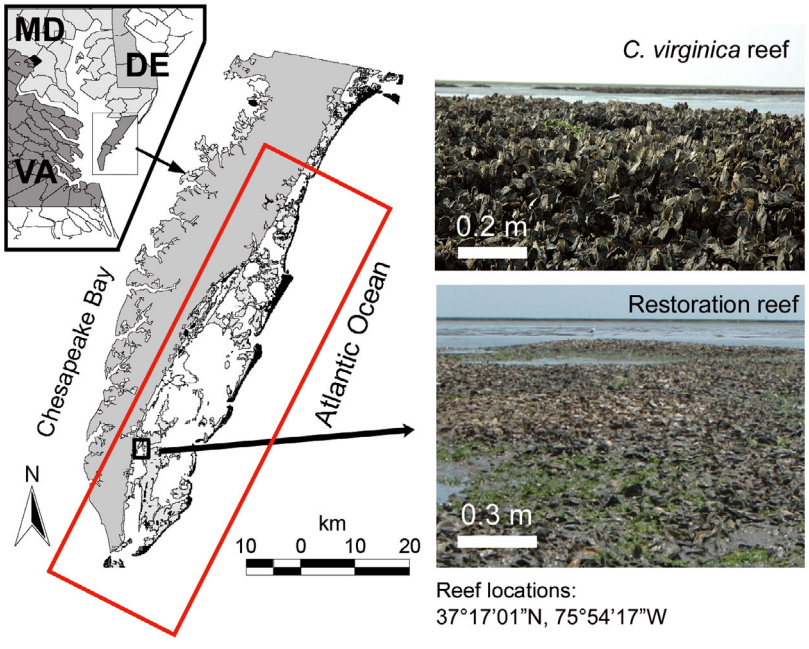

Fig. 1. Delmarva Peninsula, VA. Gray: land masses, white: water regions, and red rectangle: domain of the numerical model. Inset photos: Hillcrest oyster reef tract, including both existing *Crassostrea virginica* reefs (top) and restoration reefs (bottom). Note the difference in roughness between the *C. virginica* and the restoration reefs

gravitational sinking due to their negative buoyancy; this causes them to sink when they stop beating their cilia or retract their vela (Finelli & Wethey 2003, Koehl et al. 2007). For example, the terminal fall velocity for passive sinking of *C. virginica* was found to be 0.58 cm s^{-1} (Fuchs et al. 2013).

Although the dispersal and recruitment dynamics of marine organisms have been shown to be highly dependent upon the hydrodynamic environment (Haase et al. 2012), less is known about how these larval behaviors can influence population connectivity and the exchange of individuals among populations (Cowen & Sponaugle 2009). A major issue is that larval concentrations diminish rapidly with distance from their source location, which makes it difficult to determine the ultimate settlement location from source populations (Largier 2003). Direct measurements of larval dispersal have been performed; these include *in situ* observations of individual trajectories (Gerrodette 1981) and tagging of propagules to determine dispersal patterns (Jones et al. 2005, Almany et al. 2007, Thorrold et al. 2007). However, these techniques are labor-intensive, typically do not allow measurements of dispersal for large populations, and are location specific. For many coastal organisms, the distance of larval dispersal is directly related to the duration of the pelagic stage (Shanks et al. 2003); however, variations in the physical environment and biological behaviors create high variability in their spatial and temporal distributions. When the full range of biological behaviors of larvae cannot be completely considered, numerical models can often provide useful tools to examine subsets of biological and physical processes that contribute to specific transport outcomes (Cowen & Sponaugle 2009).

The purpose of this study is to determine how the swimming behavior of oyster larvae alter both the patterns and rates of settlement to pre-existing and to restoration oyster reefs in response to flow-mediated cues. This study used the Delft3D© numerical flow model (Deltares 2010) to evaluate hydrodynamic circulation along the Atlantic coast of Virginia, USA. The model was coupled to the Delft Water Quality particle tracking module to follow releases of larval tracers from oyster reefs and restoration sites under a range of larval settling scenarios. Larval settling was also measured *in situ* over several oyster reefs and restoration sites. Results from the model were used to investigate where larvae from individual reefs were being transported to and settle, and where self-recruitment was and was not a significant factor.

METHODS

Study site

Field and numerical studies were performed to quantify hydrodynamics and larval transport within the Virginia Coast Reserve (VCR), which is located along the eastern shore of Virginia. The VCR is characterized by a contiguous marsh, shallow bay, and barrier island system contained along ~100 km of Virginia coastline. The VCR is a site in the National Science Foundation — Long Term Ecological Research (NSF-LTER) network. Many oyster reefs can be found in the VCR, including pre-existing oyster reefs composed primarily of vertically oriented oysters and sites currently undergoing restoration (Fig. 1). A 2008 Oyster Stock Assessment Report (Ross & Luckenbach 2009; sampling between December 2007 to June 2008) estimated 3.2 billion oysters in this region, in comparison to 1.8 billion oysters for the entire Virginia portion of the Chesapeake Bay. This report provides detailed geospatial data on the location and size of pre-existing and artificial oyster reefs in the VCR region and suggests a self-sustaining population with potential for significant expansion. The Oyster Stock Assessment Report classifies oyster reefs into 5 categories: patch reefs, fringing reefs, state restoration reefs, privately managed reefs, and small patch reefs where small oyster reefs are interspersed with mud flats. To quantify larval dispersal, we selected 10 reef areas (5 of the largest reefs from both the 'patch reef' and 'state restoration reef' categories found within the VCR) described in the Oyster Stock Assessment Report (Ross & Luckenbach 2009) for particle release in our model. These reefs were respectively designated PR1 to 5 and SRR1 to 5 (Fig. 2). Most of the reefs within the VCR, including the restoration reefs, are rectangular in shape as they primarily line deeper tidal channels. Each set of 5 reefs was selected so as to have the largest total dry oyster mass in their category, as estimated by Ross & Luckenbach (2009), on the assumption that these reefs would contribute the most larvae to the seasonal spawning events (Table 1).

Mean water temperature was obtained from the VCR-LTER project datasets (www.vcrlter.virginia.edu). The data set includes water temperatures measured at 12 min intervals from the Red Bank, VA, station (Fig. 2). These temperature measurements were averaged daily from 15 May to 30 June for the period 1993–1999 and 2008 (8 yr total), as these were the only years with complete data sets for the desired time frame (Fig. 3). *Crassostrea virginica* spawn

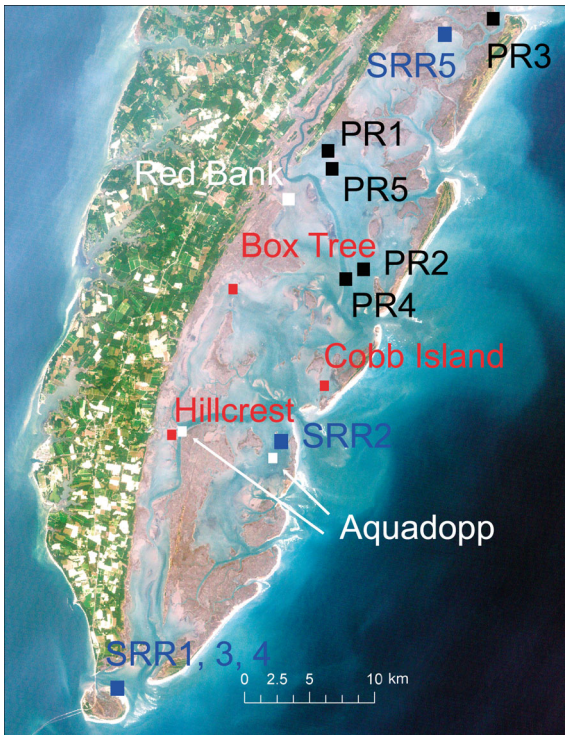

Fig. 2. Satellite photo of the Delmarva Peninsula, VA, showing the barrier islands, coastal bays and intertidal regions on the east, and the landmass (primarily farmland) on the west. Black squares: the 5 largest patch reefs (PR); blue squares: the 5 largest state restoration reefs (SRR); red squares: the Hillcrest, Cobb Island, and Box Tree reefs, where settlement plates were deployed; white squares: locations of the Aquadopp current profilers used to validate the Delft3D-Flow model. Water temperatures were recorded at Red Bank

when the water temperature reaches a daily mean value of 25°C (Galtsoff 1964). The average date when this temperature was reached during the 8 yr period of record was June 14.

Initial and boundary conditions for the hydrodynamic model

The Delft3D-Flow hydrodynamic model (Deltares®) solves the shallow-water flow equations to calculate unsteady flow and transport conditions forced by tidal and meteorological input and bottom roughness (Lesser et al. 2004). This study used a bathymetry data set compiled during previous VCR modeling studies (Mariotti et al. 2010), along with tide and wind data from NOAA meteorological stations, as input for a Delft3D-Flow simulation of the VCR coastal bay region. The bathymetry grid covers the entire VCR region (Fig. 1), with some 'buffer zone' to prevent less reliable results near the boundaries from affecting the area of interest. Each grid cell is 250 × 250 m, or 62 500 m^2.

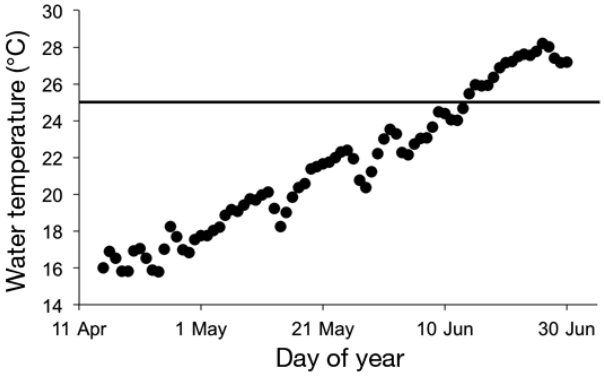

Fig. 3. Daily average water temperature measured within the Virginia Coast Reserve for the years 1993–1999 and 2008. Black line: when average water temperature reached 25°C on June 14

Water velocities are driven by local winds and tides. We used hourly wind magnitude and direction data from the NOAA monitoring station located in Wachapreague, VA (www.ndbc.noaa.gov/station_page.php?station=wahv2). The tide data sets were obtained from the Wachapreague and Chesapeake Bay Bridge Tunnel NOAA monitoring stations. The 9 most significant harmonic constituents (M2, S2, N2, K1, O1, SSA, SA, K2, P1) of these 2 stations were implemented in the model. To control the complexity and run-time of the hydrodynamic model, wind was considered to be spatially constant and flow modeling was limited to 2 dimensions, which is a reasonable simplification given the shallow water conditions of the VCR and the lack of freshwater inflows,

Table 1. Estimated total number of oysters (millions) and total dry oyster biomass (kg) of each patch reef (PR) and state restoration reef (SRR) selected for the study. Values estimated from Ross & Luckenbach (2009)

Reef	PR1	PR2	PR3	PR4	PR5	SRR1	SRR2	SRR3	SRR4	SRR5
No. of oysters (×10^6)	12.3	12.1	11.4	10.3	9.5	2.0	1.8	0.9	0.9	0.8
Total dry biomass (kg)	875	864	813	734	673	287	259	128	125	123
Reef area (m^2)	9180	9067	17930	7699	7063	3620	3270	1608	1573	1555

which limit stratification (Mariotti et al. 2010). However, the bathymetry was used as an input to the model; thus, water depth and bottom roughness, along with physical forcings of tides and winds, were all used to determine the depth averaged velocity for each grid cell within the model domain. The time step in the model is constrained by the need for computational efficiency and the Courant number (C), which is a measure of the numerical stability and accuracy of the model:

$$C = 2\Delta t\sqrt{gh\left(\frac{1}{\Delta x^2}+\frac{1}{\Delta y^2}\right)} \quad (1)$$

where Δt is the time step (s), g is standard gravity of 9.81 m s^{-2}, h is the local water depth (m), and Δx and Δy are grid lengths in the x and y directions (m). Smaller time steps have lower Courant numbers (should be <10), but are also more computationally demanding. A time step of Δt = 30 s and grid lengths Δx and Δy = 250 m were found to maintain sufficient stability in the hydrodynamic model, as evidence by reasonably low Courant numbers (<10) throughout the simulation region. The model requires a 'spin-up' time before the solutions stabilize and the model produces reliable output. A spin-up time of 5 d was included in all simulations.

Model validation

The Delft3D-Flow output was tested against field measurements from 2 Aquadopp current profilers (Nortek©) deployed on 6–14 August 2013. A representative period of 3 d (08/07/2013, 12:00 h to 08/10/2013, 12:00 h) was selected for comparison. The Aquadopps (Fig. 2), which were mounted on a frame and oriented upwards on the seafloor, measured velocity at 3 cm increments with a sampling rate of 4 Hz. The Aquadopps averaged and stored this data to internal memory every 10 min. The 3 components of velocity were measured using an internal compass in east, north, and upwards directions. The depth averaged magnitudes of the east and north components of the Aquadopp data, alongside the velocity magnitude from the model output, are plotted in Fig. 4. To quantify the relationship between the observations and the model predictions of velocity, Willmott's refined index of agreement (Willmott et al. 2012) was utilized. This index uses absolute values rather than squares, which allows greater separation for models that are performing well; it also

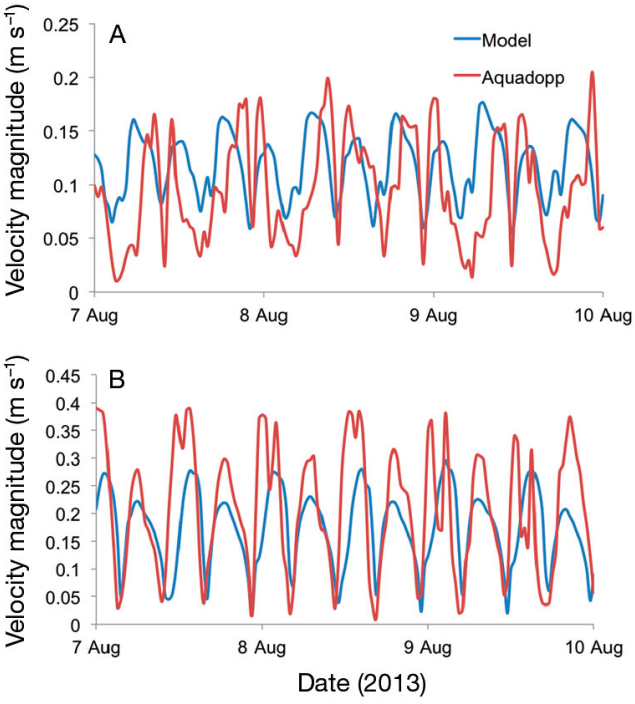

Fig. 4. Depth-averaged velocity from both the model output and the Aquadopp data, for the time period 7 August 2013 12:00 h to 10 August 2013 12:00 h. (A) Bay Aquadopp; (B) Hillcrest Aquadopp

removes model predictions from one of the terms, which means that term is an independent standard of comparison. The refined Willmott index (d_r) is given by:

$$d_r = 1-\frac{\sum_{i=1}^{n}|P_i-O_i|}{2\sum_{i=1}^{n}|O_i-\overline{O}|}, \quad \text{when} \quad \sum_{i=1}^{n}|P_i-O_i| \le 2\sum_{i=1}^{n}|O_i-\overline{O}| \quad (2)$$

$$d_r = \frac{2\sum_{i=1}^{n}|O_i-\overline{O}|}{\sum_{i=1}^{n}|P_i-O_i|}-1, \quad \text{when} \quad \sum_{i=1}^{n}|P_i-O_i| > 2\sum_{i=1}^{n}|O_i-\overline{O}| \quad (3)$$

where P_i are the model predictions, O_i are the observations, and $\overline{O}$ is the observed mean. d_r is dimensionless, ranges from –1.0 to 1.0, and is the ratio between

2 sums: the sum of the differences between the model-predicted and the observed velocities and twice the sum of the velocity deviations of the perfect model, where $P_i = O_i$ for all i (Willmott et al. 2012). The sum of the magnitudes of the observed deviations from the mean is doubled in Eq. (3) because this term also represents the behavior of a perfect model, which is equivalent to observations. When $d_r = 0$, the sum of the model errors (the difference between model predictions and observations) is equivalent to the sum of both the perfect model's deviations and the observed deviations. When $d_r = 0.5$, the sum of model errors is one-half of the sum of both the deviations of a perfect model and the deviations of the observations, while $d_r = -0.5$ indicates that the sum of the model errors is twice the sum of both the perfect model's deviations and observed deviations.

Larval tracking and behavior model

Output from the Delft3D-Flow simulation was then input to a particle-tracking algorithm called the D-Water Quality module (Deltares 2010) within the Delft3D suite of programs. This finite volume numerical model uses a Eulerian approach to solve the advection–diffusion equation on a predefined computational grid. Particle releases mimic the release and transport of *C. virginica* oyster larvae. Both the initial values of the larvae particles and the values of parameters controlling their movement may be defined in the form of a spatially varying grid (Erftemeijer et al. 2009). In this simulation, particles were used to represent oyster larvae whose swimming behavior is altered by manipulating settlement velocity, w_s (cm s^{-1}). This settlement velocity was then used to formulate a deposition flux of larvae to the seafloor, D (g cm^{-2} s^{-1}) (Deltares 2010):

$$D = w_s c \left(1 - \frac{\tau_b}{\tau_d}\right) \quad (4)$$

where c is the concentration of suspended larvae (g cm^{-3}), τ_b is bottom shear stress (Pa), and τ_d is the critical shear stress for deposition (Pa). c and τ_b were computed based on the coupled hydrodynamic output and τ_d was set to 0.1 Pa for this study, 0.1 Pa being the approximate upper limit of bed shear stress found to allow for settlement of oyster larvae (Whitman & Reidenbach 2012). w_s was adjusted to account for changes in downward swimming velocity in response to turbulence cues, thus altering the flux of larvae to the seafloor. Eq. (4) holds only when $\tau_b \leq \tau_d$, and $D = 0$ when $\tau_b > \tau_d$.

D-Water Quality allows specification of process parameters like w_s to be assigned as a spatial grid of values, so an input file was generated in which every grid cell not containing an oyster reef was assigned one value for w_s, and grid cells containing an oyster reef or restoration site could be assigned a different value. Fuchs et al. (2013) observed that downward vertical velocities for swimming oyster larvae ranged between 1.8 cm s^{-1} in strong turbulence to near-zero values in still water; for $\varepsilon > 0.071$ cm^2 s^{-3}, larvae actively propelled themselves downward using a diving behavior, where downward swimming velocity increased with elevated ε. Mean flow and turbulence dissipation characteristics over oyster reefs, restoration sites, and bare seafloor composed of sand-silt sediment were previously quantified by Whitman & Reidenbach (2012). Although ε varied with velocity for a given bed roughness, an analysis of the data showed that for water velocities of ~15 cm s^{-1} (similar to mean water column averages measured over oyster reefs, restoration sites and mudflats; Whitman & Reidenbach 2012), mean ε was 1.97 ± 0.41 cm^2 s^{-3} over oyster reefs, 0.21 ± 0.05 cm^2 s^{-3} over restoration sites, and 0.05 ± 0.01 cm^2 s^{-3} over mud. This indicates that under mean flow conditions, dissipation was typically below the threshold to induce active sinking over bare seafloor and was greatest over the most hydraulically rough substrate (oyster reefs), with dissipation being large enough to induce active sinking. In the model, $w_s = 1.8$ cm s^{-1} was used to represent typical settlement velocities over existing reef areas which induce high turbulence, w_s = 0.9 cm s^{-1} was used to represent the settlement velocity over restoration reef areas, and $w_s = 0.02$ cm s^{-1} was used as the low, non-reef, near neutral buoyancy settlement velocity expected during the larval planktonic stage or when over bare seafloor. These are similar to conditions applied in Fuchs & Reidenbach (2013).

As it is a finite-volume model, D-Water Quality handles particles in terms of mass per volume for suspended particles, or mass per area for deposited particles. To simulate the mass of an actual oyster spawning event, the total mass of oyster larvae spawned from a reef needs to be specified. Each female *C. virginica* oyster releases ~50–60 million eggs per spawning season; released ova and sperm are then mixed in the water column where fertilization occurs (Carriker 1951). Approximately 1 d after fertilization, larvae are ~60 µm in diameter and can swim actively; they continue to grow for the next 2 wk to the eyed larval stage. At this stage, shells of competent larvae are ~300 µm in diameter, with a

mean density of 1.15 ± 0.02 g cm^{-3} (Fuchs et al. 2013). Assuming a roughly spherical shape, each larva has a mass of ~1.63×10^{-5} g once competent. Because the proportion of eggs that are fertilized is dependent on local conditions and mortality is expected to be high during the larval stage (MacInnes & Calabrese 1979, Elston & Leibovitz 1980, Baker & Mann 1992), it is not possible to predict the quantity of larvae (larvae m^{-2}) that will reach competency from a given reef with much accuracy. To normalize findings so that results are independent of larval release densities, the results of each simulation were quantified as the ratio (or percentage) of total settled larvae relative to settlement rates from a different larval release scenario modeled within this study. In the present study, the magnitudes of releases were adjusted to broadly account for variation in reef size. Based on the data from Ross & Luckenbach (2009), the largest patch reefs were ~10× larger than the largest state restoration reefs (Table 1). Therefore, all simulations were configured so that 30 g of larval particles were released from each of the patch reefs and 3 g of larval particles were released from each of the restoration reefs. Assuming each larva to weigh 1.63×10^{-5} g upon reaching competency, this is equivalent to the release of ~2×10^6 larvae (30 g/1.63×10^{-5} g per larva = 1.84×10^6 larvae) from each of the patch reefs, and ~2×10^5 competent larvae (3 g/1.63×10^{-5} g per larva = 1.84×10^5 larvae) from each of the restoration reefs. These numbers are likely on the low end of actual rates of larval production; however, for modeling purposes, each simulated particle trajectory can represent the path of thousands of larvae (North et al. 2008). In addition, mortality of larvae, which would likely reduce the overall rate of successful settlement to reefs, was not modeled. However, under the assumption that mortality is not correlated with pelagic swimming behavior, this would not affect model results which compare the ratio between total settled larvae relative to settlement rates obtained from a simulation with different initial or boundary conditions.

Before larvae reach maturity, which takes ~14 d (the age at which transition to pediveliger occurs), they are not viable to colonize reefs (Carriker 1951); thus, for the first 14 d, a near neutral buoyancy of w_s = 0.02 cm s^{-1} is expected to occur everywhere. All simulations consisted of 2 parts: a 14 d period when larvae are in their planktonic stage, followed by a 7 d period when larvae are allowed to preferentially settle. The specific simulations performed were grouped into 2 categories. The first set of runs consisted of 8 simulations designed to examine the degree to which larval swimming behavior affects settlement rates and patterns. Various settlement conditions were tested, including over bare seafloor, oyster reefs, and restoration sites (Table 2). In each of these simulations, the larval particles were released simultaneously over all 10 reefs on 14 June 2013. Although multiple larval releases of *C. virginica* larvae may occur throughout the year (Loosanoff 1966), this model focused on the early summer release. Larval release was simulated to occur gradually over a period of 6 h, from 12:00 h to 18:00 h on 14 June, and transport of larvae from the reefs only occurred when reefs were submerged. Mass spawning events of *C. virginica* larvae typically take place over a period of hours to days (Ingle 1951), so this was deemed a reasonable length of discharge.

The second set of simulations sought to determine the dispersal characteristics of oyster larvae and the origin of larvae that ultimately settle. Simulations were performed in which particles were released from each patch reef individually (PR1–PR5). Although releases only occurred from one patch reef, these simulations were identical to B8 in all other respects (14 d with w_s = 0.02 cm s^{-1}, followed by 7 d with w_s = 1.8 cm s^{-1} only over patch reefs and w_s = 0.9 cm s^{-1} only over restoration reefs). Once the model was calibrated and tested, larval dispersal was modeled across the time period of 6 June 2013 through 13 July 2013. This time frame allowed spin-up time and substantial margin of time surrounding the 3 wk time period for the simulations (13 June 2013 to 5 July 2013). For all simulations, the larval concentration on the seafloor from the final time step was produced and retrieved as a map file across the entire grid to represent total larval settlement rates for the duration of the spawn.

Table 2. Simulations performed with uniform settlement velocity (w_s) during the initial 14 d during pre-competent planktonic stage (Days 0–14), followed by varying w_s during the following 7 d of settlement while competent (Days 15–21)

Simulation	w_s pre-competent (cm s^{-1})	w_s competent (cm s^{-1})		
		Over bare seafloor	Over restoration sites	Over oyster reefs
B1	0.02	0.02	0.02	0.02
B2	0.9	0.9	0.9	0.9
B3	1.8	1.8	1.8	1.8
B4	0.02	0.9	0.9	0.9
B5	0.02	0.02	0.9	0.9
B6	0.02	1.8	1.8	1.8
B7	0.02	0.02	1.8	1.8
B8	0.02	0.02	0.9	1.8

In situ larval settlement rates

To determine *in situ* larval settlement rates, larval settlement plates constructed of slate tiles were deployed and left in place between 10 June and 2 August 2014, which is within the typical spawning and settlement time periods of oyster larvae from June through September (Kennedy & Krantz 1982). Settlement plates were deployed at an oyster restoration site and an adjacent existing oyster reef site at 3 locations: Hillcrest, Cobb Island, and Box Tree oyster reef sites (Fig. 2). At each of the 6 locations (3 restoration sites and 3 pre-existing oyster reefs), 7 settlement plates were deployed, consisting of a total tile surface area of 0.18 m^2. Each plate ranged in size between 0.3 × 0.05 m to 0.3 × 0.3 m. Plates placed on the top of pre-existing reefs were, if possible, situated in areas which allowed for the plates to be within interstices between oysters and thus below the very top of the reef. The larval settlement plates at the restoration sites were deployed on top of deposited oyster shell, ~100 to 200 m from the settlement plates deployed on the oyster reefs. After retrieval of the settlement plates, total oyster spat (>1 mm diameter) was counted.

RESULTS

Typical model velocities under flood and ebb tide conditions ranged between near-zero to 0.4 m s^{-1} within the coastal bays, with overall mean flows of ~0.10 m s^{-1} (Fig. 5). Within these coastal bays, ebb and flood conditions are approximately symmetric. Velocities tend to be highest in the inlet channels between the barrier islands that shelter the VCR, with peak velocities of ~0.5 m s^{-1}. Further offshore, modeled currents are slightly higher in the open ocean during ebb (0.15 to 0.2 m s^{-1}) as compared to inshore waters.

The amplitudes of the velocity fluctuations at the off-shore Aquadopp site deployed in South Bay were slightly greater than the model predictions for the 3 d period (Fig. 4A), while the mean velocities were roughly similar. A Willmott index of d_r = 0.517 was found for this site. The near-shore Aquadopp (Fig. 4B), deployed adjacent to the Hillcrest oyster site and situated along a tidal channel, showed better agreement with the model output, with a Willmott index of d_r = 0.550. These Willmott index values indicate that the sum of the model errors is roughly one-half of the sum of both the deviations of the perfect model and the deviations of observations. At both deployment sites, the timing of the tides can be assumed to cause most of the deviation of observations from the observed mean, and these index values suggest that the overall magnitude of the model error is similar to the overall magnitude of the deviations in the observations caused by the tides.

Larval dispersal patterns

To determine how modifications in swimming behavior alter rates of larval settlement to reef habitat, simulations were initially run with a constant w_s across the entire 21 d period (simulations B1, B2, and B3). Total settlement increased by more than one order of magnitude (Table 3) with an increase in w_s from 0.02 to 0.9 cm s^{-1} (comparing average larval settlement between simulations B1 and B2), and by almost 2 orders of magnitude when w_s was increased from 0.02 to 1.8 cm s^{-1} (comparing simulations B1 and B3). Although this increase is substantial, total settlement to reefs increased even further when larvae initiated settlement only when competent (i.e. after their 14 d planktonic stage), with an average additional increase of 5.3% from B2 to B4 (w_s = 0.9 cm s^{-1}), and an 11.0% increase from B3 to B6 (w_s = 1.8 cm s^{-1}). Fig. 6 shows settlement patterns of larvae, with

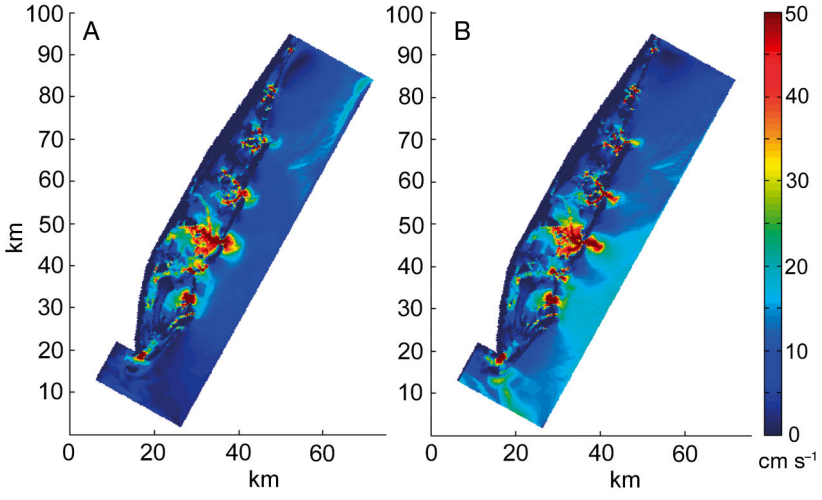

Fig. 5. Depth-averaged velocity (cm s^{-1}) throughout the Virginia Coast Reserve for (A) flood tide and (B) ebb tide. Colors on the figure indicate velocity magnitude, while the axes (in km) indicate location within the model domain

Table 3. Average larval density (g m^{-2}) on all reefs for the set of simulations B1 to B8, which examine the effects of changes in larval swimming behavior on settlement patterns. w_s: settlement velocity; pre-competent planktonic stage: Days 0–14; competent stage: Days 15–21. w_s = 0.02, 0.9, and 1.8 cm s^{-1} are low, medium and high settlement velocities, respectively

Simulation	w_s pre-competent (cm s^{-1})	w_s competent (cm s^{-1})	Average larval settlement density (g m^{-2})
B1	Low	Low	2.36×10^{-7}
B2	Medium	Medium	9.91×10^{-6}
B3	High	High	1.85×10^{-5}
B4	Low	Medium	1.04×10^{-5}
B5	Low	Medium over reefs, low elsewhere	1.06×10^{-5}
B6	Low	High	2.05×10^{-5}
B7	Low	High over reefs, low elsewhere	2.12×10^{-5}
B8	Low	High over patch reefs, medium over restoration reefs, low elsewhere	2.04×10^{-5}

w_s = 0.02 cm s^{-1} during the initial 14 d planktonic period, followed by w_s = 0.02, 0.9, or 1.8 cm s^{-1} at all locations, during the 7 d period when larvae are competent to settle. It should be noted that simulations B1, B2, and B3 are ecologically unrealistic because larvae do not settle during their pre-competency period. They were run as a comparison to determine how having this pre-competent period, when larvae are free-swimming (Runs B4–B8), extends the dispersal distance of larvae.

Table 3 includes settlement rates when increased settlement velocities occur only over existing reefs (Simulations B7 and B8). These results illustrate how larval behavior has a substantial effect on the magnitude and location of settlement. Overall, compared to remaining at near-neutral swimming behavior of w_s = 0.02 cm s^{-1}, behavioral changes in swimming patterns, where competent larvae increase w_s to 1.8 cm s^{-1} when over existing reefs, increased the accumulation of larvae by almost 2 orders of magnitude (B1 compared to B7). Settlement onto oyster reefs increased by almost 40× for the medium settlement velocities of w_s = 0.9 cm s^{-1} that are expected to occur over restoration sites. This indicates that waiting to initiate settlement until after the 14 d planktonic stage, and preferentially settling only over hard substrate (either existing or restoration oyster sites), offer a substantial increase in the probability of successful recruitment. Settlement velocities for simulation B8, where w_s = 0.9 cm s^{-1} over restoration sites and 1.8 cm s^{-1} over patch reefs, showed slightly less larval settlement than when w_s = 1.8 cm s^{-1} over all reefs (B8 compared to B7). This is expected and indicates that the majority of larval settlement is occurring over the patch reefs. The simulations were not able to represent the larval behavior of upward swimming to re-suspend themselves if they settle on undesirable substrate. For this reason, it is likely that actual settlement would be somewhat higher at all locations in simulations B4 and B6, and somewhat higher over reefs in simulations B5, B7, B8, and PR1–5, as discussed below.

Results from simulations that only included larval release from a single patch reef (Fig. 7) indicate that the highest concentrations of larvae have settled in regions around their initial release, indicating substantial self-recruitment of the patch reefs (Table 4; see Fig. 2 for the locations of the various patch reefs). Examination of settlement on the same reef that larvae were released from shows that all of the reefs either received more of their total accumulation from

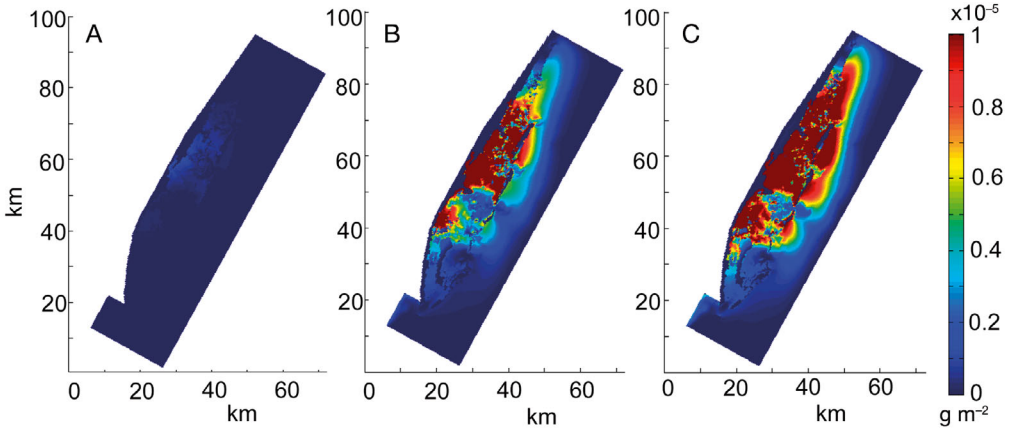

Fig. 6. Color-coded maps of total larval settlement density (g m^{-2}) for simulations (A) B1, (B) B4, and (C) B6, each having a w_s = 0.02 cm s^{-1} settlement velocity for 14 d during the planktonic stage, but with varying settlement velocities (w_s = 0.02, 0.9, and 1.8 cm s^{-1}, respectively) during the subsequent 7 d of settlement. Colors on the figure indicate larval settlement density, while the axes (in km) indicate location within the model domain

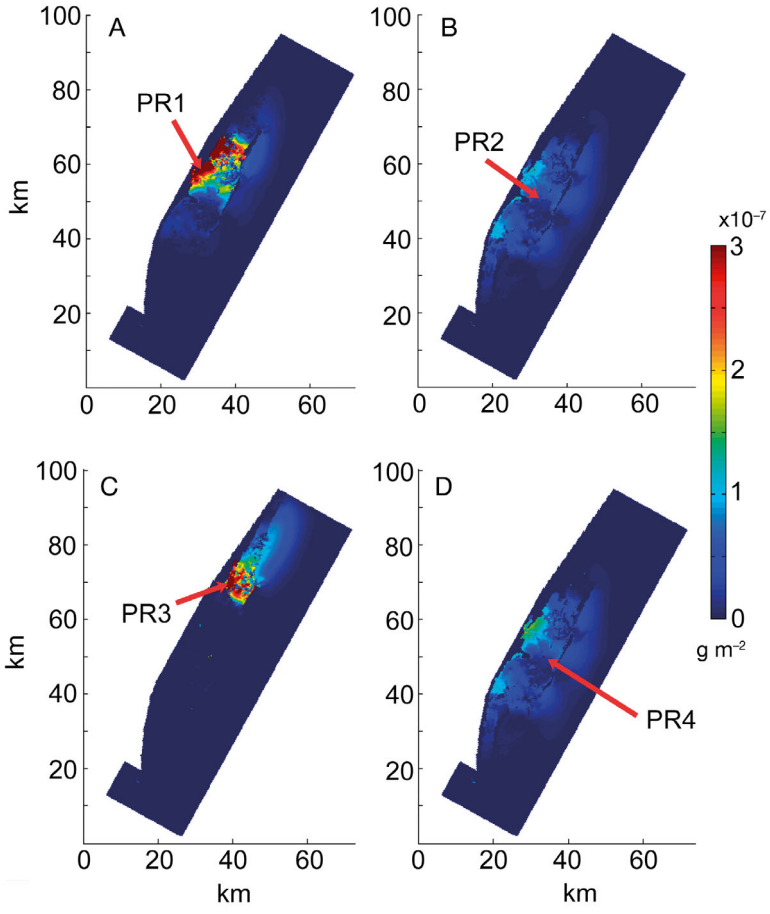

Fig. 7. Total larval settlement density (g m^{-2}) at the end of each simulation implementing larval release at a single patch reef: (A) PR1, (B) PR2, (C) PR3, and (D) PR4. Red arrow marks location of originating reef. PR5 (not shown) is located adjacent to PR1 and has similar dispersal characteristics. Colors on the figure indicate larval settlement density, while the axes (in km) indicate location within the model domain

Table 4. Larval settlement from releases of larvae originating from Reefs PR1 to PR5, utilizing model simulations where 30 g of larvae were released from just that reef. Column 2 shows the settlement of larvae (g m^{-2}) originating from that reef onto all 10 reefs in the model domain. % of larvae from self-recruitment: the amount of the total settlement onto the originating reef that was from self-recruitment; % of total larval supply to all reefs: the relative amount of larvae that was supplied to all reefs from the originating reef

Reef	Larval settlement (g m^{-2})	Larvae from self-recruitment (%)	Total larval supply to all reefs (%)
PR1	6.67×10^{-6}	36.4	31.5
PR2	2.71×10^{-6}	25.5	12.8
PR3	1.52×10^{-6}	81.4	7.2
PR4	3.34×10^{-6}	28.4	15.8
PR5	6.79×10^{-6}	36.6	32.1

their own release than from any other reef, or the contribution from their own release was ranked 2nd. In addition, each reef tended to receive more larvae from nearby reefs than from more distant reefs. Lastly, depending upon both location and total larval release, some patch reefs contributed much more to the larval settlement on neighboring reefs than others. Overall, reefs PR1 and PR5 contributed the most larvae, while PR3 contributed <10% of its spawned load to the 10 reefs in the model.

The settlement resulting from larval releases from reefs PR2 and PR4 is spread over a larger area as compared to settlement contributed by reefs PR1, PR3, and PR5 and also includes more deposition outside the barrier islands (Fig. 7). Regions within the model domain containing oyster reefs have significantly higher settlement than surrounding non-reef regions. Settlement seems to roughly vary inversely with velocity (Fig. 5), as might be expected, since higher larval settlement generally occurs in areas of lower velocity due to lower rates of dispersal.

In situ larval settlement

Larval settlement densities quantified using settlement plates show large differences in total recruitment depending upon reef location and benthic substrate within the VCR (Table 5). Total larval settlement measurements indicate that the greatest settlement occurred on reefs at Hillcrest at 22 700 ± 3000 larvae m^{-2}, with settlement rates being ~3× lower on the Cobb Island and Box Tree reefs. Values provided in the table are the means (±1 SD) of larval settlement (spat of 1 mm diameter or greater) onto the 7 settlement plates located on each of the restoration sites or oyster reefs. The Hillcrest reef site is the most interior and protected of the 3 sites and is exposed to the lowest-flow conditions. This site also had the greatest existing oyster population of the 3 sites (Ross & Luckenbach 2009). At each of the 3 measurement locations, settlement to restoration reef areas was approximately half of that found on pre-existing reefs at the same site, with the greatest recruitment of 12 000 ± 4900 larvae m^{-2} at the Hill-

Table 5. Larval settlement (larvae m^{-2} ± 1SD) onto settlement plates located on oyster reefs and adjacent restoration sites at 3 locations within the Virginia Coastal Reserve, as shown in Fig. 2

	Cobb Island	Hillcrest	Box Tree
Pre-existing oyster reef	7600 ± 3300	22 700 ± 3000	7200 ± 3400
Restoration site	2800 ± 1700	12 000 ± 4900	4400 ± 700

crest oyster restoration site. The numerical model released larvae from only the 5 largest existing patch reefs and the 5 largest restoration reefs. Given that there are hundreds to thousands of existing reefs within the model domain, poor agreement of larval settlement between the model and *in situ* measurements is expected. However, there is good qualitative agreement in larval settlement results between the numerical model and the *in situ* measurements, particularly in terms of the relative settlement rates found between existing and restoration sites, as well as between site locations.

DISCUSSION

Larval transport and reef connectivity

Results from the hydrodynamic simulations show that the flow environment in the bays protected by the barrier islands and containing most of the oyster reefs in this region are relatively calm, with mean flows of ~0.10 to 0.15 m s^{-1}. Flows through the deep channels that are connected to the inlets separating the barrier islands are dominated by high velocities reaching 0.5 m s^{-1}. Connectivity of oyster populations throughout the VCR depends upon oyster larvae transport within these faster channel currents, combined with larval dispersal within the bays. Due to these variable flows, larval dispersal greatly depends upon source location.

The distribution of larval settlement locations obtained from simulations B1–B8 (Fig. 7) shows that most larvae do not settle very far from their original spawning location. Many of the existing reefs and restoration sites are found in interior bays, and velocity maps (Fig. 5) indicate low velocities around many of these spawn points, which indicates that larvae will both tend to stay in these bays and settle there more readily than they will elsewhere due to purely physical (non-behavioral) processes. Reefs located further from the mainland towards the barrier islands show substantially enhanced larval dispersal. The numerically computed velocities through these deeper channels indicate substantially faster flows between the barrier islands; this should drive significant transport in the vicinity of and through these inlets, including transport of larvae into the open ocean (out of the model domain). Larvae that are transported into the open ocean are not likely to survive due to the lack of hard substrates to settle on in these deeper ocean environments.

The present results are similar to that of a numerical study of population dynamics conducted in North Carolina (Haase et al. 2012), which showed high non-uniformity in larval connectivity between broodstock reserves. Initial release locations of larval particles influenced both the spread and the distance traveled by larvae over a 14 to 21 d period, and potential settlement areas varied according to the location of the natal reserve, even without including behavior within the 'virtual' larvae. The results shown in our model suggest that both the local hydrodynamic environment and swimming behavior can have a substantial impact on spatial dispersal patterns. Linked to this is the extent to which these populations are open or closed: open populations receive and export individuals to other populations, while closed populations do not exchange individuals and primarily rely on self-recruitment (Warner & Cowen 2002, Wieters et al. 2008, Cowen & Sponaugle 2009). Within the VCR, the closer source populations are to high velocity tidal channels or to outer bay regions near the barrier islands, the more open is the population. However, this may come at a cost of reduced overall concentrations of larvae available to populate new areas due to enhanced dispersal. Under low oyster populations and reduced reef area, closed populations may ultimately fair better because of increased larval settlement densities to existing reefs. Therefore, the extent of connectivity between reefs within the VCR, and the location of the reefs, likely influence the structure and dynamics of these populations (Cowen et al. 2000).

Larval settlement model

Numerical simulations show that changes in larval behavior that increase downward swimming velocities over existing reefs are an effective means of enhancing the rate of transport and deposition of larvae onto reefs, thereby increasing larval settlement densities. Total settlement of larvae (Table 3) responded very strongly to increasing values of w_s, with a nearly 100-fold increase when settlement velocity

was 1.8 cm s^{-1} compared to near-neutral swimming during pre-competency. The values presented in Table 3 also show that the 14 d pre-competency period not only allows larvae to mature, but substantially increases their dispersal distance as compared to larvae that might settle within the first 14 d of life (simulations B2 and B3). For larvae selectively increasing their settlement velocity only while over existing reefs as compared to other sites, accumulation of larvae onto suitable habitat increased by 3.0% for high settlement velocities (w_s = 1.8 cm s^{-1}). This somewhat small increase is primarily due to the low proportion of oyster reef area compared to total seafloor area; as reef area expands, the relative amounts of larvae reaching suitable habitat should also increase. Thus, this indicates 2 drawbacks to having a low surface area of suitable settlement habitat: low amounts of hard, stable benthic surface area for oysters to settle and grow, and low source populations from which new larvae are produced. This combination reduces both the number of larvae in the water column and the probability that an individual larva will encounter a suitable settlement habitat. These results suggest that by selectively avoiding settling in regions not identified as suitable reef habitat, larvae in the water column leave greater populations that are able to settle when they are carried over suitable substrate.

Influence of reef roughness and turbulence on settlement

Our model quantitatively shows that larval responses to enhanced water column turbulence over oyster reefs, whereby oyster larvae actively swim towards the seafloor, increase the rate of settlement onto hard substrate. Studies by Whitman & Reidenbach (2012) showed that mean estimates of the drag coefficient, C_D (used as a measure of hydrodynamic roughness), over a *Crassostrea virginica* reef were 2× greater than over oyster restoration sites and 5× greater than over bare seafloor. This drag enhanced both peak Reynolds stresses and vertical momentum transport above the reef, injecting turbulence into the overlying water column. A strong shear layer also developed within the mean velocity profile above the oyster reef, contributing to the production of turbulent kinetic energy. Although enhanced turbulence can solely be a major contributor to settlement on reefs, Fuchs & Reidenbach (2013) utilized a spatial 'hitting-distance' larval transport model to identify habitat characteristics that jointly maximized both the settlement probability and the density of recruits on the scale of individual reefs. Larvae settled most successfully when diving over rough substrates in shallow water, and settlement probabilities were higher on larger reef patches, although average settler densities were higher on smaller reef patches. Water depth was the greatest source of variability in terms of delivery of competent larvae to a reef, followed by larval behavior, substrate roughness, and then water velocities. Our results, in combination with Fuchs & Reidenbach (2013), suggest that increasing reef area and oyster populations will certainly increase both larval numbers and successful settlers; however, optimal sizing and location of oyster reefs are dependent upon local water depth and current speed, as well as how the substrate roughness might impact larval behavior.

This strong velocity shear, in combination with elevated turbulence levels, can also have a substantial effect on the transport and mixing of dissolved chemical cues (Koehl & Reidenbach 2007, Koehl et al. 2007, Reidenbach et al. 2007), which may be used by larvae to induce settlement (Tamburri et al. 1996). Higher roughness and faster mean flows were found to increase the rate of transport of chemical cues from the substratum, although increased levels of turbulence tend to more rapidly mix these cues within the water column, causing an overall reduction in concentrations. However, few studies have looked at the combined effects of turbulence and chemical cue structure on the timing and spatial extent of larval settlement. Such interactions may ultimately be important in the settlement of oyster larvae.

When modeled settlement velocities of 0.9 cm s^{-1} (those expected over restoration reefs) are used, the rate of deposition of larvae onto reefs is approximately half that of settlement using w_s = 1.8 cm s^{-1} (those expected over pre-existing oyster reefs composed of more vertically oriented oysters). This agrees with *in situ* larval settlement measurements that found a 1.5 to 3-fold increase in larval settlement onto settlement plates placed on existing reefs compared to settlement plates on restoration reefs. This suggests that additional turbulence cues that initiate greater behavioral responses can substantially increase settlement onto reefs. However, in addition to the turbulence cues generated by the reef, the complex 3-dimensional structure provides physical and biological refugia for larvae, and micro-scale variations in location and elevation within the substrate can strongly affect settlement processes (Bartol & Mann 1997, Bartol et al. 1999). The high-roughness vertical surfaces found on patch reefs may also pro-

vide refuge from predation and sedimentation (Grabowski 2004, Schulte et al. 2009). Although turbulence cues induce settlement to reefs, the enhanced near-bed flow and shear stresses induced by rough topography can reduce rates of successful settlement by washing away larvae that have not adequately attached to the substrate (Crimaldi et al. 2002, Reidenbach et al. 2009, Koehl & Hadfield 2010). Whitman & Reidenbach (2012) found that although area averaged fluid shear may be greater on *C. virginica* reefs, local turbulence and shear stresses within interstices between oysters were reduced and can provide adequate refuge for successful settlement. These near-bed flow effects, in addition to predation and post-settlement mortality, may have also altered the settlement of larvae onto the settlement plates. It should be noted that results presented by Wheeler et al. (2013) found that larvae had a propensity to actively swim upward in high turbulence and not exhibit a downward directed swimming response. This result is opposite to that found by Fuchs et al. (2013) and Finelli & Wethey (2003), and occurred over the same range of energy dissipation rate; however, the experiments by Wheeler et al. (2013) were conducted in a grid-stirred turbulence tank that produced near-isotropic turbulence. This turbulence lacks the strong vertical shear experienced by larvae within the bottom boundary layer over oyster reefs (Whitman & Reidenbach 2012). Although more studies are needed, a shear flow that creates a vertical velocity gradient, in addition to elevated turbulence levels, may be needed to ultimately trigger a downward swimming response in larvae, and may explain the discrepancy between swimming behavior found within an open-channel flow (Finelli & Wethey 2003) and that found within a grid-stirred tank (Wheeler et al. 2013).

Influence of reef location on settlement

The results shown in Table 4 indicate that self-colonization constitutes a major fraction of the overall settlement onto reefs. This is further demonstrated by the result of simulation B8, in which the restoration reefs were assigned a lower settlement velocity than the patch reefs. The average larval recruitment was only marginally less than that in simulation B7, where both reef types had a high settlement velocity, indicating that factors aside from settlement velocity, specifically reef location, are controlling recruitment at the restoration reefs. Colonization generally took place more often between reefs located in close proximity than between those further apart, although there was clearly more connectivity between some reefs than others. Reefs PR1 and PR5, which are closer to shore in slower flow regions, showed the highest percentage of average contribution to all of the reefs in the model; PR2, PR3, and PR4, which were further offshore and closer to the higher velocity channels, showed lower average contributions. Due to their location near the high flow tidal channels, larvae from PR2, PR3 and PR4 had larger overall dispersal ranges, as well as significant transport out of the bays to the open ocean. The very low contribution of PR3 (7.2%) can also partially be explained by its relatively greater distance from the rest of the reefs, and general northward flow direction, which transports larvae away from existing reef areas.

The larval settlement maps shown in Fig. 7 also demonstrate that areas of low velocity near the shore trap a great deal of larvae, keeping them from dispersing to other regions. For these reefs, larval connectivity with other regions within the VCR is probably not important to attain enough colonizing larvae for survival, and larval transport is unlikely to be a limiting factor in reef growth. Other reefs located in a higher velocity environment do not contribute a significant quantity of larvae to their immediate vicinity and therefore likely require larvae from other, possibly distant, reefs to sustain themselves. These reefs can be assumed to be much more dependent on the connectivity between various regions within the VCR, and growth may be limited by the quantity of larvae they receive each season.

In situ larval settlement densities utilizing settlement plates qualitatively agreed with the findings from the numerical studies regarding settlement location, where reefs located inland in slower-moving waters containing relatively large populations of oysters (Hillcrest reef site) had significantly greater recruitment than reefs found either further offshore (Cobb Island) or in higher-flow environments (Box Tree). Interior reefs with large existing oyster populations that are exposed to lower-flow conditions have greater self-recruitment and total recruitment than reefs exposed to higher velocities and higher rates of larval dispersal.

Model limitations

The comparison between the *in situ* Aquadopp observations and model velocity predictions showed significant deviation of predictions from observa-

tions. There are several factors that may explain the magnitude of these errors. First, the spatial heterogeneity present in a 250 × 250 m grid cell cannot be assumed to be accurately represented at a single point within that grid cell. In the case of the Aquadopp deployed near the Hillcrest oyster reef, the flow effects of the oyster reef may not be representative of area averaged velocity of that grid cell, which might explain why the model consistently underestimated observed velocities at this site. Second, it appears that in the case of the off-shore Aquadopp, the tidal fluctuations predicted by the model were slightly out of phase with those observed, which significantly increased the error shown by the Willmott index. Larval settlement was examined over several days, and error in the tidal phase of the model is unlikely to significantly affect overall settlement numbers.

Model accuracy is also constrained by the quality of the inputs. Winds are expected to be heterogeneous over such a large region, but wind data was only available at one point, which was extrapolated to the entire model domain. Also, the bay bathymetry was derived from compilations of airborne LIDAR (VITA 2011; mostly topographic data) and sonar bathymetry datasets, in addition to local surveys and NOAA charts (Mariotti et al. 2010). In some regions, data was interpolated to ensure that the channels and bay system were well represented. These issues should affect the entire model domain to the same degree; therefore, while the actual values of larval settlement will be affected, the patterns of larval transport and comparisons of settlement under different behavior conditions are still valid. Finally, a limitation in the formulation of the model was that it was not 3-dimensional, and water depths and bottom friction, along with tidal and meteorological forcings, were used to compute the depth averaged horizontal velocity. Velocity shear and variability in turbulence with height above the substratum have been shown to significantly affect the ability of larvae to land and successfully settle, both in oyster reefs (Whitman & Reidenbach 2012) and in other coastal systems such as coral reefs (Reidenbach et al. 2009). The location where larvae reside vertically within the water column can also fundamentally alter dispersal patterns. However, due to the shallow (often 1 m or less), non-stratified conditions found within the VCR, the depth averaged velocity was determined to be a good predictor for bulk flow and dispersal patterns of larvae, but may not adequately determine the settlement success of larvae once they reach the seafloor.

CONCLUSION

Our results indicate that basic behavioral decisions by larvae regarding swimming or sinking in response to turbulence cues can have a dramatic effect on larval distributions and rates of settlement onto suitable benthic habitat. Model simulations effectively show that larval swimming behavior (i.e. swimming to stay in the water column until mature and over a suitable reef) does substantially improve their chances of settling on a reef, thus increasing rates of survivorship. Our simulations also effectively demonstrate where cohorts of larvae from different reefs ultimately settle and that reefs found in protected, low-flow regions within the VCR have much greater levels of self-recruitment.

Acknowledgements. We thank Barry Truitt, Bowdoin Lusk and The Nature Conservancy for access to oyster reefs and restoration sites. M. Kremer provided field assistance with the larval settlement plates, and P. Wiberg offered valuable assistance with the Delft-3D model and comments on the manuscript. This research was supported by a grant to M.A.R. (NSF-OCE 1151314) and Virginia Coast Reserve Long Term Ecological Research grants (NSF-DEB 0621014 and DEB 1237733) provided by the National Science Foundation.

LITERATURE CITED

Almany GR, Berumen ML, Thorrold SR, Planes S, Jones GP (2007) Local replenishment of coral reef fish populations in a marine reserve. Science 316:742–744

Baker S, Mann R (1992) Effects of hypoxia and anoxia on larval settlement, juvenile growth, and juvenile survival of the oyster *Crassostrea virginica*. Biol Bull 182:265–269

Bartol IK, Mann R (1997) Small-scale settlement patterns of the oyster *Crassostrea virginica* on a constructed intertidal reef. Bull Mar Sci 61:881–897

Bartol IK, Mann R, Luckenbach ML (1999) Growth and mortality of oysters (*Crassostrea virginica*) on constructed intertidal reefs: effects of tidal height and substrate level. J Exp Mar Biol Ecol 237:157–184

Breitburg DL, Coen LD, Luckenbach MW, Mann R, Posey M, Wesson JA (2000) Oyster reef restoration: convergence of harvest and conservation strategies. J Shellfish Res 19:371–377

Butman CA (1987) Larval settlement of soft-sediment invertebrates: the spatial scales of pattern explained by active habitat selection and the emerging role of hydrodynamical processes. Oceanogr Mar Biol Annu Rev 25:113–165

Carriker MR (1951) Ecological observations on the distribution of oyster larvae in New Jersey estuaries. Ecol Monogr 21:19–38

Cerco CF, Noel MR (2007) Can oyster restoration reverse cultural eutrophication in Chesapeake Bay? Estuaries Coasts 30:331–343

Cowen RK, Sponaugle S (2009) Larval dispersal and marine population connectivity. Annu Rev Mar Sci 1:443–466

Cowen RK, Lwiza KM, Sponaugle S, Paris CB, Olson DB

(2000) Connectivity of marine populations: open or closed? Science 287:857–859

Crimaldi JP, Thompson JK, Rosman JH, Lowe RJ, Koseff JR (2002) Hydrodynamics of larval settlement: the influence of turbulent stress events at potential recruitment sites. Limnol Oceanogr 47:1137–1151

Deltares (2010) Delft3D-Flow user manual. Deltares, Delft

DiBacco C, Fuchs HL, Pineda J, Helfrich K (2011) Swimming behavior and velocities of barnacle cyprids in a downwelling flume. Mar Ecol Prog Ser 433:131–148

Eckman JE, Werner FE, Gross TF (1994) Modelling some effects of behavior on larval settlement in a turbulent boundary layer. Deep-Sea Res II 41:185–208

Elston R, Leibovitz L (1980) Pathogenesis of experimental vibriosis in larval American oysters, *Crassostrea virginica*. Can J Fish Aquat Sci 37:964–978

Erftemeijer PLA, van Beek JKL, Bolle LJ, Dickey-Collas M, Los HFJ (2009) Variability in transport of fish eggs and larvae. I. Modelling the effects of coastal reclamation. Mar Ecol Prog Ser 390:167–181

Finelli CM, Wethey DS (2003) Behavior of oyster (*Crassostrea virginica*) larvae in flume boundary layer flows. Mar Biol 143:703–711

Fuchs HL, Reidenbach MA (2013) Biophysical constraints on optimal patch lengths for settlement of a reef-building bivalve. PLoS ONE 8:e71506

Fuchs HL, Mullineaux LS, Solow AR (2004) Sinking behavior of gastropod larvae (*Ilyanassa obsoleta*) in turbulence. Limnol Oceanogr 49:1937–1948

Fuchs HL, Hunter EJ, Schmitt EL, Guazzo RA (2013) Active downward propulsion by oyster larvae in turbulence. J Exp Biol 216:1458–1469

Galtsoff PS (1964) The American oyster *Crassostrea virginica* (Gmelin). US Fish Wildl Serv Fish Bull 64:1–480

Gerrodette T (1981) Dispersal of the solitary coral *Balanophyllia elegans* by demersal planular larvae. Ecology 62:611–619

Grabowski JH (2004) Habitat complexity disrupts predator–prey interactions but not the trophic cascade on oyster reefs. Ecology 85:995–1004

Haase AT, Eggleston DB, Luettich RA, Weaver RJ, Puckett BJ (2012) Estuarine circulation and predicted oyster larval dispersal among a network of reserves. Estuar Coast Shelf Sci 101:33–43

Hadfield MG, Koehl MAR (2004) Rapid behavioral responses of an invertebrate larva to dissolved settlement cue. Biol Bull 207:28–43

Hidu H, Haskin H (1978) Swimming speeds of oyster larvae *Crassostrea virginica* in different salinities and temperatures. Estuaries 1:252–255

Ingle RM (1951) Spawning and setting of oysters in relation to seasonal environmental changes. Bull Mar Sci 1: 111–135

Jones GP, Planes S, Thorrold SR (2005) Coral reef fish larvae settle close to home. Curr Biol 15:1314–1318

Kemp WM, Boynton WR, Adolf JE, Boesch DF and others (2005) Eutrophication of Chesapeake Bay: historical trends and ecological interactions. Mar Ecol Prog Ser 303:1–29

Kennedy VS (1996) Biology of larvae and spat. In: Kennedy VS, Newell RIE, Eble AF (eds) The eastern oyster *Crassostrea virginica*. Maryland Sea Grant Publication, College Park, MD, p 371–421

Kennedy V, Krantz L (1982) Comparative gametogenic and spawning patterns of the oyster *Crassostrea virginica* (Gmelin) in central Chesapeake Bay. J Shellfish Res 2: 133–140

Koehl MAR, Hadfield M (2010) Hydrodynamics of larval settlement from a larva's point of view. Integr Comp Biol 50: 539–551

Koehl MAR, Reidenbach MA (2007) Swimming by microscopic organisms in ambient water flow. Exp Fluids 43: 755–768

Koehl MAR, Strother JA, Reidenbach MA, Koseff JR, Hadfield MG (2007) Individual-based model of larval transport to coral reefs in turbulent, wave-driven flow: behavioral responses to dissolved settlement inducer. Mar Ecol Prog Ser 335:1–18

Largier JL (2003) Considerations in estimating larval dispersal distances from oceanographic data. Ecol Appl 13:71–89

Lenihan HS, Peterson CH (1998) How habitat degradation through fishery disturbance enhances impacts of hypoxia on oyster reefs. Ecol Appl 8:128–140

Lesser G, Roelvink J, Van Kester J, Stelling G (2004) Development and validation of a three-dimensional morphological model. Coast Eng 51:883–915

Loosanoff VL (1966) Time and intensity of setting of the oyster, *Crassostrea virginica*, in Long Island Sound. Biol Bull 130:211–227

MacInnes JR, Calabrese A (1979) Combined effects of salinity, temperature, and copper on embryos and early larvae of the American oyster, *Crassostrea virginica*. Arch Environ Contam Toxicol 8:553–562

Mariotti G, Fagherazzi S, Wiberg P, McGlathery K, Carniello L, Defina A (2010) Influence of storm surges and sea level on shallow tidal basin erosive processes. J Geophys Res: Oceans 115:C11012, doi:10.1029/2009JC005892

Nelson KA, Leonard LA, Posey MH, Alphin TD, Mallin MA (2004) Using transplanted oyster (*Crassostrea virginica*) beds to improve water quality in small tidal creeks: a pilot study. J Exp Mar Biol Ecol 298:347–368

Nestlerode JA, Luckenbach ML, O'Beirn FX (2007) Settlement and survival of the oyster *Crassostrea virginica* on created oyster reef habitats in Chesapeake Bay. Restor Ecol 15:273–283

Newell RI (1988) Ecological changes in Chesapeake Bay: Are they the result of overharvesting the American oyster, *Crassostrea virginica*? Understanding the estuary: advances in Chesapeake Bay research. Chesapeake Bay Res 129:536–546

North EW, Schlag Z, Hood RR, Li M, Zhong L, Gross T, Kennedy VS (2008) Vertical swimming behavior influences the dispersal of simulated oyster larvae in a coupled particle-tracking and hydrodynamic model of Chesapeake Bay. Mar Ecol Prog Ser 359:99–115

Reidenbach MA, Koseff JR, Monismith SG (2007) Laboratory experiments of fine-scale mixing and mass transport within a coral canopy. Phys Fluids 19:075107

Reidenbach MA, Koseff JR, Koehl MAR (2009) Hydrodynamic forces on larvae affect their settlement on coral reefs in turbulent, wave-driven flow. Limnol Oceanogr 54:318–330

Reidenbach MA, Berg P, Hume A, Hansen JC, Whitman ER (2013) Hydrodynamics of intertidal oyster reefs: the influence of boundary layer flow processes on sediment and oxygen exchange. Limnol Oceanogr Fluids Environ 3:225–239

Ross PG, Luckenbach MW (2009) Population assessment of eastern oysters (*Crassostrea virginica*) in the seaside

coastal bays. Final Report to the Virginia Coastal Zone Management Program, Richmond, VA. Virginia Institute of Marine Science, College of William and Mary, Wachapreague, VA

Rothschild BJ, Ault JS, Goulletquer P, Héral M (1994) Decline of the Chesapeake Bay oyster population: a century of habitat destruction and overfishing. Mar Ecol Prog Ser 111:29–39

Schulte DM, Burke RP, Lipcius RN (2009) Unprecedented restoration of a native oyster metapopulation. Science 325:1124–1128

Shanks AL, Grantham BA, Carr MH (2003) Propagule dispersal distance and the size and spacing of marine reserves. Ecol Appl 13:159–169

Tamburri MN, Finelli CH, Wethey DS, Zimmer-Faust RK (1996) Chemical induction of larval settlement behavior in flow. Biol Bull 191:367–373

Thorrold S, Zacherl D, Levin L (2007) Population connectivity and larval dispersal using geochemical signatures in calcified structures. Oceanogr 20:80–89

Turner EJ, Zimmer-Faust RK, Palmer MA, Luckenbach ML, Pentcheff ND (1994) Settlement of oyster (*Crassostrea virginica*) larvae: effects of water flow and water-soluble chemical cue. Limnol Oceanogr 39:1579–1593

VITA (2011) LIDAR-based Digital Elevation Model for Northampton and Accomack Co., VA, 2010. Long Term Ecological Research Network. http://dx.doi.org/10.6073/pasta/b5a7c766f864637b8ebfbf316d8bd5fa (accessed 20 August 2015)

Warner RR, Cowen RK (2002) Local retention of production in marine populations: evidence, mechanisms, and consequences. Bull Mar Sci 70:245–249

Wheeler JD, Helfrich KR, Anderson EJ, McGann B and others (2013) Upward swimming of competent oyster larvae *Crassostrea virginica* persists in highly turbulent flow as detected by PIV flow subtraction. Mar Ecol Prog Ser 488:171–185

Whitman ER, Reidenbach MA (2012) Benthic flow environments affect recruitment of *Crassostrea virginica* larvae to an intertidal oyster reef. Mar Ecol Prog Ser 463: 177–191

Wieters EA, Gaines SD, Navarrete SA, Blanchette CA, Menge BA (2008) Scales of dispersal and the biogeography of marine predator–prey interactions. Am Nat 171:405–417

Willmott CJ, Robeson SM, Matsuura K (2012) A refined index of model performance. Int J Climatol 32:2088–2094

Wood LH, Hargis WJ (1971) Transport of bivalve larvae in a tidal estuary. Cambridge University Press, London

Editorial responsibility: Romuald Lipcius, Gloucester Point, Virginia, USA

Submitted: October 17, 2014; Accepted: May 27, 2015
Proofs received from author(s): August 21, 2015